Dynamic Response and Power Production of an Integrated Offshore Renewable Energy System

Liang Li, Zhiming Yuan, Yan Gao
Department of Naval Architecture, Ocean and Marine Engineering, University of Strathclyde
100 Montrose Street, Glasgow, United Kingdom

ABSTRACT

This study investigates the dynamics and energy production of a new offshore floating renewable energy system, which integrates an offshore floating wind turbine (OFWT), a wave energy converter (WEC) and two tidal turbines. The hybrid concept is proposed to enhance the energy production through the combination of the three types of renewable energy systems. Simulation results show that the combined concept achieves a synergy between the floating wind turbine, the wave energy converter and the tidal turbines. Compared with a single floating wind turbine, the combined concept undertakes reduced surge and pitch motions. The overall power production increases by approximately 15%.

KEY WORDS: Renewable energy; offshore floating wind turbine; wave energy converter; tidal turbine; dynamic response.

INTRODUCTION

Due to the issues like environmental pollution, energy crisis and sustainable development, the exploitation of offshore energy is boosted by the global pursuit of renewable energy. Coastal areas provide the renewable energy sources in the form of wind, sea currents, and waves. Theories and technologies have been developed to exploit these types of offshore renewable energy resources.

Over the last decade, a large number of offshore floating wind turbine concepts have been developed. Statoil Nielsen et al. (2006) proposed a SPAR-buoy floating wind turbine, namely the Hywind concept, which is the first full-scale floating wind turbine that has ever been built. Principle Power installed a full-scale 2MW WindFloat prototype near the coast of Portugal (Principle Power, 2017). Hu et al. (2016) investigated the dynamics of a semi-submersible floating wind turbine during normal operation state and emergency shutdown. Li et al. (2018a) measured the dynamic response of a floating wind turbine in experimental environment. Cheng et al. (2017b) numerically examined the dynamics of a vertical axis floating wind turbine.

Compared to wind, wave energy is a renewable resource with high power density and all-day availability. WECs with various operation mechanisms have been proposed. Zhang and Yang (2015) studied the power capture of a heaving point absorber in both regular and irregular waves. Henriques et al. (2016) enlarged the energy absorption of an oscillating-water-column WEC with latching control strategy. Babarit et al. (2017) utilized pressure-different mechanism to extract energy from the sea waves.

Sea current is gradually accepted as a solution to the sustainable generation of electrical power. The majority of tidal turbine designs are based on horizontal axis turbines, similar to those applied in the wind energy industry. Bahaj et al. (2007) used blade element momentum (BEM) theory to predict the hydrodynamic performance of a horizontal axis tidal turbine in steady flow and compared the predicted results with experimental measurement. Zhang et al. (2015) studied how the hydrodynamic performance of a tidal turbine was affected when installed on a floating platform. They revealed a positive correlation between the oscillation amplitude and the frequency of platform surge motion.

In a site where wind, waves and sea currents coexist, the combination of a floating wind turbine, a wave energy converter and a tidal turbine may be a prospective and economical solution to the full exploitation of offshore renewable energy. Some studies on the combined deployment of wind, wave and tidal energy have been conducted and reported by previous researchers. Aubault et al. (2011) incorporated an oscillating-water-column type WEC into a semi-submersible floating wind turbine. Muliawan et al. (2013) studied the dynamic response and the power performance of a combined SPAR-type floating wind turbine and coaxial floating wave energy converter in operational conditions. Further experimental and numerical studies of the hybrid concept in survival mode were conducted (Wan et al., 2015). Michailides et al. (2014) incorporated a flap-type WEC to a semi-submersible floating wind turbine and investigated the effect of WECs on the response of the integrated system. Bachynski and Moan (2013) studied the effects of 3 point absorber WECs on a TLP floating wind turbine in operational and 50-year extreme environmental conditions, in terms of power take-off, structural loads and platform motions. Li et al. (2018b) incorporated a WEC and tow tidal turbines to a spar-type floating turbine. It was shown that the platform motions were reduced and the overall energy production was enhanced.

The hybrid concept proposed in Li et al. (2018b) is considered in this study. Aero-hydro-mooring coupled simulations are performed to investigate the performance of the HWNC, in terms of platform motions, power production and mooring line tension. No control scheme is applied in the modelling. It will examine whether the performance of the HWNC can be improved with the installation of the WEC and the tidal turbines.

CONCEPT DESCRIPTION

The combined concept is inspired by the SPAR-type floating wind turbine Hywind (Jonkman, 2010), the two-body floating WEC ‘Wavebob’ and the NACA 638xx airfoil series. The WEC, designed to move only in heave mode relative to the platform, is connected to the

platform through mechanical facilities. Two tidal turbines are installed to harvest energy from the sea current. The main dimensions of the HWNC are presented in Table 1 and the inertial properties of each component are listed in Table 2. Compared with the initial design, these parameters are somewhat adjusted.

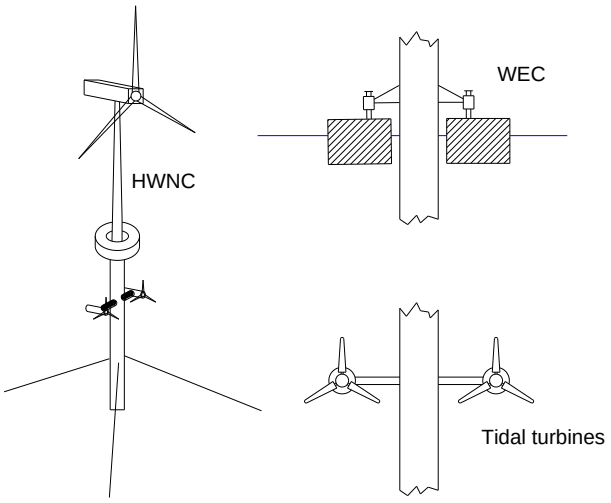

Fig. 1. HWNC concept.

Table 1 Main dimensions of the HWNC

	Item	Value
Platform	Draft	120 m
	Depth to top of taper	4 m
	Depth to bottom of taper	12 m
	Platform diameter above taper	6.5 m
	Platform diameter above taper	9.4 m
WEC	Draft	4 m
	Outer diameter	20 m
	Inner diameter	10 m
Tidal turbine	Depth	46.5 m
	Rotor diameter	10 m

Table 2 Inertial properties

	Item	Value
Platform	Total mass	6.995E+06 kg
	Centre of mass (CM) below SWL	89.9 m
	Roll inertia about CM	4.229E+09 kg·m^2
	Pitch inertia about CM	4.229E+09 kg·m^2
	Yaw inertia about CM	1.642E+08 kg·m2
WEC	Total mass	1.442E+06 kg
	CM below SWL	0 m
	Roll inertia about CM	3.139E+06 kg·m^2
	Pitch inertia about CM	3.139E+06 kg·m^2
	Yaw inertia about CM	6.022E+06 kg·m^2

Table 3 Mooring line properties

Item	Value
Depth to anchors	320 m
Depth of fairleads	70 m
Radius to anchors	853.87 m
Radius to fairleads	5.2 m
Unstretched mooring line length	902.2 m
Mooring line diameter	0.09 m
Equivalent mooring line mass density	77.7066 kg/m

NUMERICAL MODELING AND VALIDATION

The numerical simulation tool is based on the combination of WindSloke developed by Li et al. (2015) and WEC-Sim (WEC-Sim, 2017) developed under the collaboration between the National Renewable Energy Laboratory (NREL) and the Sandia National Laboratories.

The wind force is computed by a modified blade element momentum (BEM) method. The unsteadies of the inflow caused by platform motions is considered with a dynamic wake model (Bramwell et al., 2001). The so-called induced velocity is first calculated with the blade element method, and then filtered by the dynamic model. The filtered value will be used to calculate the local drag and lift forces acting on the blade element. The same method is used to compute the tidal turbine thrust forces.

WEC-Sim is a wave energy converter simulation tool with the ability to model offshore systems that are comprised of rigid bodies, PTO systems and mooring systems. The PTO system is numerically treated as a spring & damper system. The stiffness coefficient K is set to 5 kN and the damping coefficient B is set to 80 kN·s/m. The mooring line is modelled with the lumped-mass approach, which divides the mooring line into a series of evenly-sized segment represented by connected nodes and spring-damper systems. Potential flow theory is used to address the hydrodynamics, and the memory effect of free water surface is considered using the retardation kernel.

Since the thrust forces acting on the wind turbine and the tidal turbines are simulated with the same approach, only aerodynamic force is validated here. Firstly, the steady aerodynamic performance is validated, and the results are shown in Fig. 2. As shown, the agreement is good.

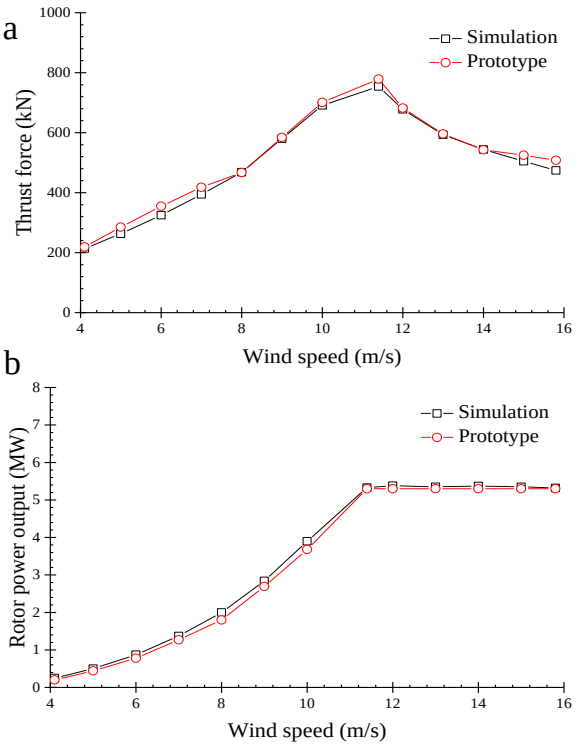

Fig. 2. Aerodynamic performance of the wind turbine. (a) thrust force; (b) rotor power output.

Due to the platform motions, the aerodynamic loads acting on the wind turbine are unsteady. To validate the unsteady aerodynamic

performance, the wind turbine thrust force is simulated under a set of sinusoidal winds and the simulation results are compared with those obtained by FAST (Jonkman and Buhl Jr, 2005). The speed of sinusoidal wind is defined by

$$V(t) = V_0 + \sin(\omega t) \quad (1)$$

where V_0 is the average wind speed and ω is the varying frequency. The control module in FAST is switched off so that the rotor speed and the blade pitch angle are fixed in the simulations. Fig. 7 displays time series of the unsteady wind turbine thrust forces predicted by the simulation tool and FAST.

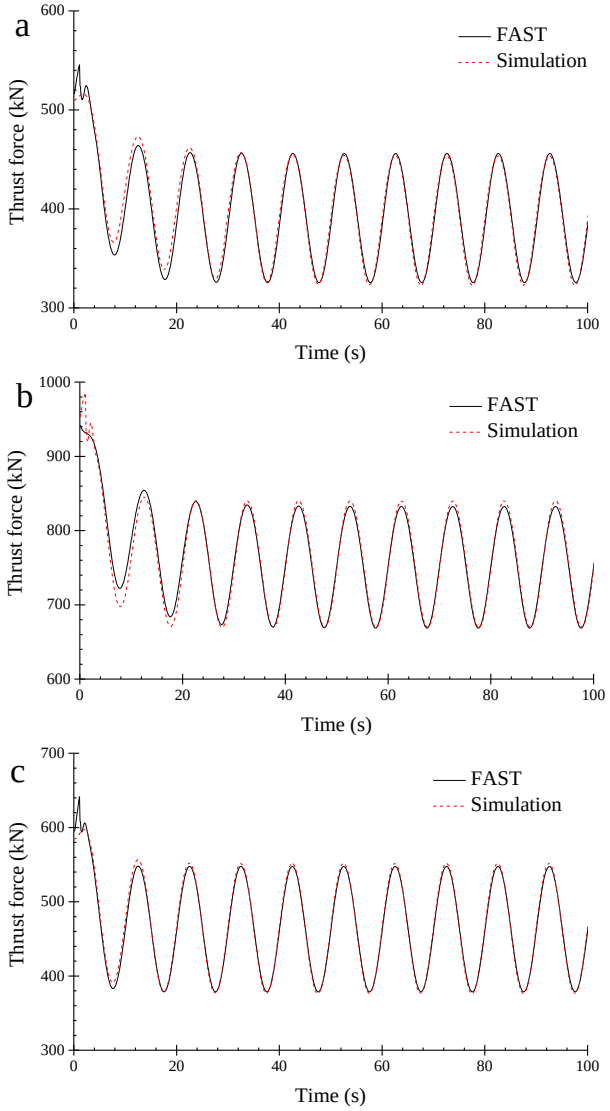

Fig. 3. Times series of unsteady wind turbine thrust forces. (a) V_0 = 8 m/s, ω = 0.63rad/s; (b) V_0 = 11.4 m/s, ω = 0.63 rad/s; (c) V_0 = 14 m/s, ω = 0.63 rad/s.

The model test of a spar type floating wind turbine conducted by Koo et al. (2014) is used to validate the numerical modelling of platform-wind turbine couplings. The spar type floating wind has an in identical platform geometry with the Hywind, but with different inertial properties. More information of the model set-up can be found in (Koo et al., 2014). White noise waves were generated in the model test to get the response amplitude operator (RAO) of platform motions in the presence of rated wind turbine thrust force. The same procedure is employed in the numerical simulation. Fig. 4 compares the RAOs acquired by the simulation tool and the experiment. Good agreement with experimental measurement is obtained.

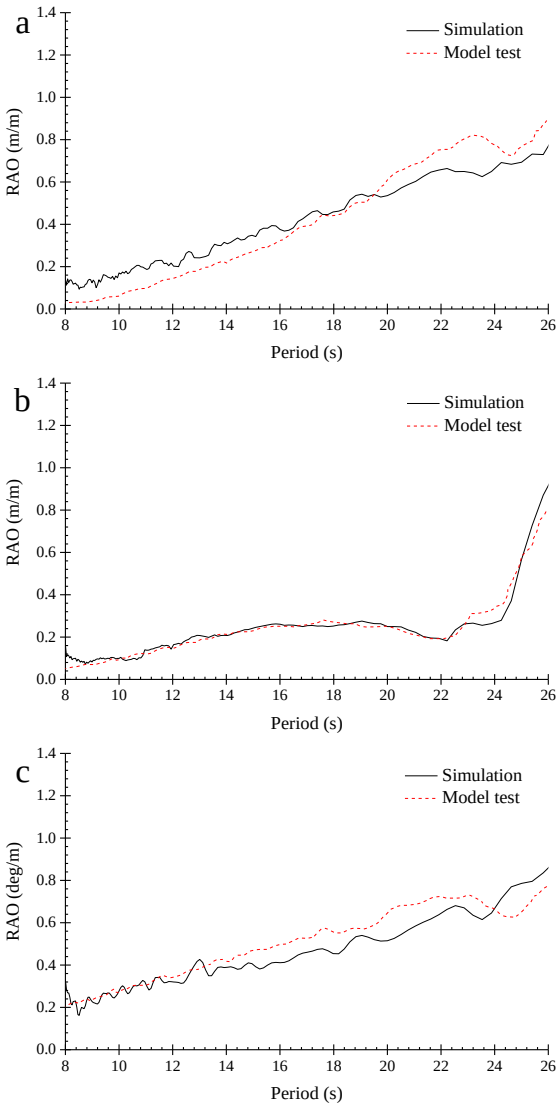

Fig. 4. RAOs of platform motions. (a) surge motion; (b) heave motion; (c) pitch motion.

SIMULATION RESULTS

Table 4 Environmental conditions

Wave condition		Wind velocity	Sea current speed
H_s	T_p		
3.13 m	10.17 s	11.4 m/s	1 m/s

This section will examine the dynamic performance of the HWNC, in terms of platform motions, power production and mooring line tension. Comparison will be made with the Hywind to elaborate whether the performance of the HWNC can be improved with the incorporation of the other two energy systems. The environmental conditions considered in the simulations are listed in Table 4. The waves, wind and sea currents all propagate along negative X direction. Only uniform wind is considered. The irregular incident waves are described with the Pierson Moskowitz spectrum.

Platform Motions

Table 5 summaries the statistics of platform motions. The equilibrium position of the platform is varied with the action of sea current force. Meanwhile, the average inclined angle of the platform is somewhat changed as well. Fig. 5 displays the power spectrum density (PSD) of the platform motions. It is shown that the HWNC performs better in terms of surge and pitch motions. The reduced surge and pitch motions are beneficial since reduced platform motion lead to stable wind turbine power output.

Table 5 Statistical results of platform motions

		Max	Mean	Min	Std. dev
Surge (m)	HWNC	-28.9	-30.0	-31.0	0.34
	Hywind	-24.1	-25.4	-26.7	0.38
Heave (m)	HWNC	-0.1	-0.4	-0.9	0.15
	Hywind	-0.1	-0.4	-0.6	0.08
Pitch (deg)	HWNC	-3.5	-4.0	-4.5	0.15
	Hywind	-3.5	-4.1	-4.7	0.18

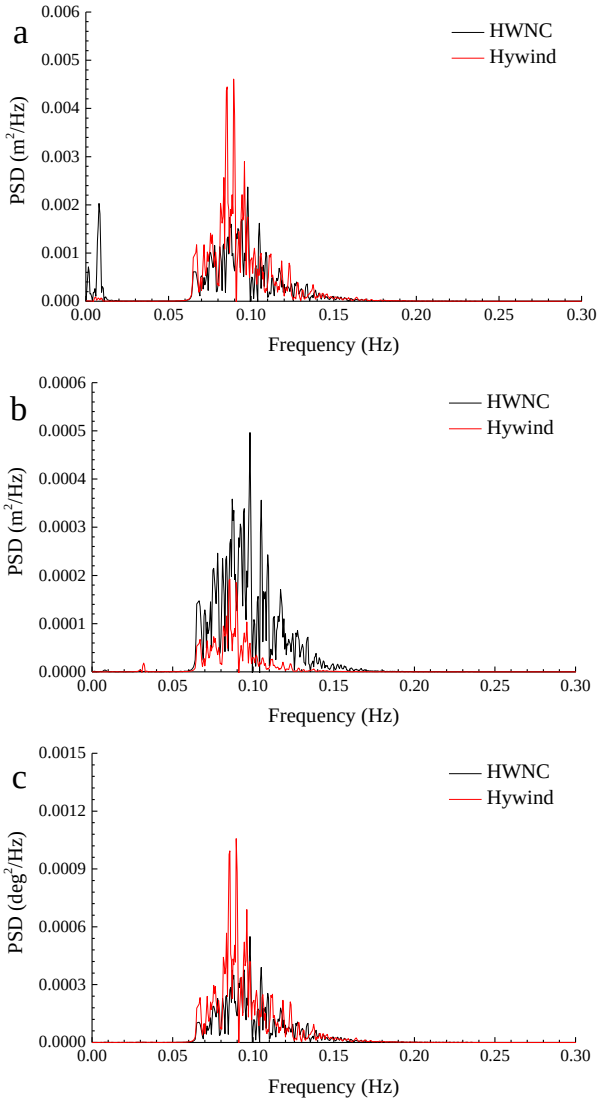

Fig. 5. PSD of platform motions. (a) surge motion; (b) heave motion; (c) pitch motion.

The reduction of surge and pitch motions is partially attributed to the tidal turbines, which produce an extra damping. Since the sea current propagates along negative X direction, the thrust force acting on the tidal turbine rotor can be approximated by

$$T(\dot{x}) = -C_T \cdot \frac{1}{2}\rho\pi R^2 (U_0 + \dot{x})^2 \tag{2}$$

where C_T is the thrust force coefficient, U_0 the is sea current speed. Applying Taylor expansion at $\dot{x} = 0$, the following series is derived,

$$T(\Delta\dot{x} + 0) = T(0) - C_T\rho\pi R^2 U_0 \Delta\dot{x} - C_T\rho\pi R^2 U_0 \Delta\dot{x}^2 + O(\Delta\dot{x}^2) \tag{3}$$

The first term is a constant component, which only influences the mean position of the platform. The third term is of second-order and can be regarded as small compared to the first-order term. The second term is a damping term which helps to reduce the platform motions. Eq. (3) illustrates that although the tidal turbine thrust force pushes the platform more far from the initial equilibrium position and may induce larger mooring line tension, it produces a damping component which helps to reduce the platform motions.

Despite that surge and pitch motions are reduced, is unfavorable to see that the heave motion is amplified. The increased heave motion is mainly attributed to the installation of WEC, which augments the water plane area of the system significantly. It means that the vertical wave excitation force applying on the system will become much larger. Although the increased heave motion will have limited influence on the wind turbine power output, it is very likely to lead to unfavorable structural force at critical connections, such as the tower base and the tower top.

Power Production

Fig. 6 plots the times series of HWNC power output. As shown, the contributions from the WEC and tidal turbines are considerable. The statistical results of the power production are summarized in Table 6. The wind turbine power production of the HWNC is hardly reduced. Please note that the rotor power production is used here, which is 5.5 WM at rated operational state. Besides, wind turbine control is not considered. Compared with the Hywind, the total power production of the HWNC is increased by roughly 15%. Moreover, the standard deviation of wind turbine power production is reduced.

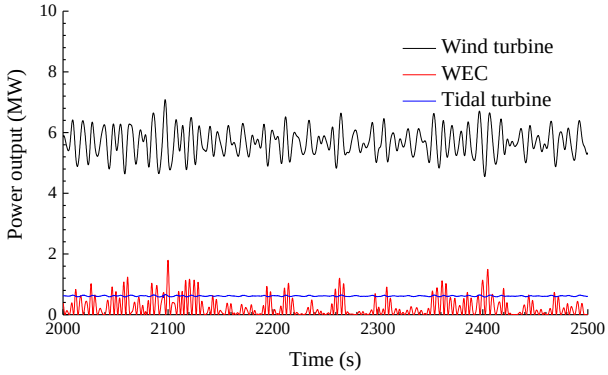

Fig. 6. Times series of power output of the HWNC.

Table 6 Statistical results of power production.

	HNCW			Hywind
	Wind	Wave	Tide	
Mean (MW)	5.68	0.25	0.61	5.68
Std. dev (MW)	0.43	0.34	0.01	0.50

Considering that surge and pitch motions are reduced with the installation of the WEC and the tidal turbines, the unsteadiness of the inflow seen by the HWNC should become less significant accordingly.

Therefore, the wind turbine energy production will become more stable. It is also proved by the FFT analysis result in Fig. 7. As shown, the spectra peak value of the HWNC is much lower than that of the Hywind. The spectra peak is observed around 0.1Hz, namely the peak period of the incident wave. It indicates that the unsteadiness of the inflow is mainly caused by the inertial motions of the platform. Although the average wind turbine power output of the HWNC is not increased, it is favorable to see the improvement of the power output quality. A stable wind turbine power output is beneficial to the grid.

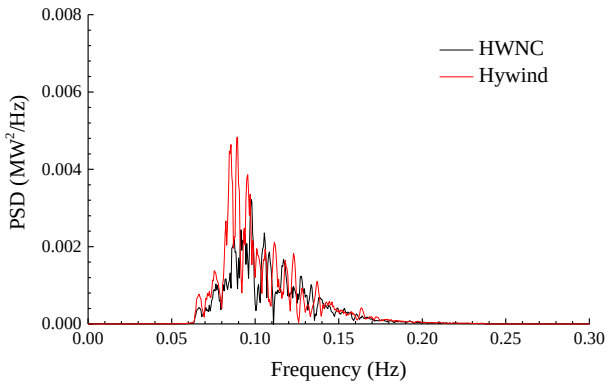

Fig. 7. PSD of wind turbine power production.

Mooring Line Tension

Fig. 8 plots the time-series of mooring line tension force and Table 7 summaries the statistical results. The mean tension is increased by approximately 10% due to the sea current force. Besides, it can be found that the mooring line fluctuation of the HWNC is stronger than that of the Hywind. It has been pointed out that the surge and pitch motions of the HWNC are reduced while the heave motion is amplified. Consequently, the amplified mooring line dynamic response is attributed to the increased heave motion of the platform. Since the extreme response is dominated by the mean force and the oscillating component, the extreme tension force increased as well. It is obviously a negative aspect of the installation of the tidal turbines.

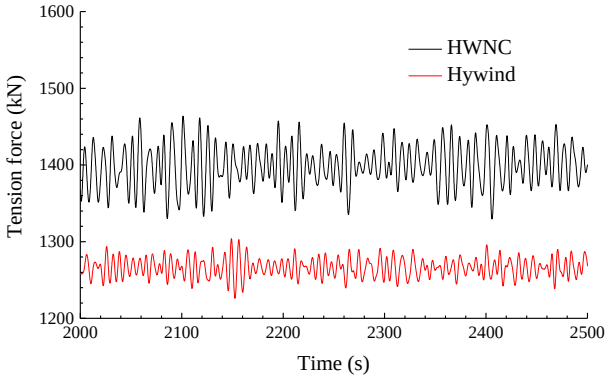

Fig. 8. Time series of mooring line tension.

Table 7 Statistics of mooring line tension

	Max (kN)	Min (kN)	Mean (kN)	Std.dev(kN)
HWNC	1482	1303	1399	27.3
Hywind	1304	1226	1266	11.5

To further investigate the short-term extreme response of the mooring line, the up-crossing rate of mooring lien tension force is calculated. To investigate the tail region behavior (corresponding to low very low up-crossing rate), the fitted method used in (Cheng et al., 2017a) is adopted here. Fig. 9 illustrates that the mooring line of HWNC is more likely to subject to large tension force due to the thrust forces acting on the tidal turbines.

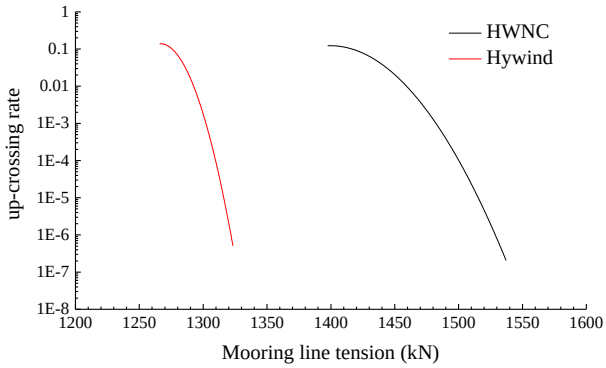

Fig. 9. Up-crossing rate of mooring line tension.

Although the platform motions (surge and pitch modes) and the power output of HWNC is improved, the dynamic response of mooring line increases and the maximum tension reaches a very high level. The current mooring system which is designed for a single floating wind turbine is proved not suitable for the HWNC concept. A new mooring system must be specially designed for the HWNC, which should be able to undertake very large tension. More importantly, the fatigue loads must be carefully considered in the design due to the increased standard deviation of mooring line tension.

CONCLUSION

We proposed a new offshore renewable energy system by integrating a floating wind turbine, a wave energy convector and two tidal turbines, with the primary objective to enhance the power production ability and reduce the motions at the same time. Aero-hydro-mooring coupled analysis is performed in time domain to investigate the platform motions, power production and mooring line tension of the hybrid concept. Based on the numerical results, the following conclusions are drawn:

Due to the damping force produced by the tidal turbines, the surge and pitch motions of the platform are reduced. The wind turbine power output becomes more stable in the presence of reduced platform motions. In spite of the reduced surge and pitch motions, the heave motion of HWNC is increased. The negative effect induced by the amplified heave motion should be further investigated.

With the WEC and the tidal turbines, the overall power production of the HWNC could be increased by roughly 15%. The average power production of the wind turbine is hardly varied at the same time. Due to reduced platform surge and pitch motions, the quality of wind turbine power production was enhanced.

It was found that the mean tension of a mooring line was increased due to the current forces acting on the tidal turbines. Additionally, the standard deviation of the tension increased significantly with the installation of the WEC and the tidal turbines. The mooring system, which is initially designed for a single floating wind turbine, may be not applicable to the HNWC. Further study should be performed on the improvement of the mooring system.

REFERENCES

NWTC Information Portal (WEC-Sim), 2017,

https://nwtc.nrel.gov/WEC-Sim/.

Aubault, A, Alves, M, Sarmento, A, Roddier, D, and Peiffer, A (2011). "Modeling of an oscillating water column on the floating foundation WindFloat," *International Conference on Ocean, Offshore and Arctic Engineering*, American Society of Mechanical Engineers, 235-246

Babarit, A, Wendt, F, Yu, YH, and Weber, J (2017). "Investigation on the energy absorption performance of a fixed-bottom pressure-differential wave energy converter," *Appl. Ocean Res*, 65, 90-101.

Bachynski, EE, and Moan, T (2013). "Point absorber design for a combined wind and wave energy converter on a tension-leg support structure," *International Conference on Ocean, Offshore and Arctic Engineering*, American Society of Mechanical Engineers, V008T009A025-V008T009A025

Bahaj, A, Batten, W, and McCann, G (2007). "Experimental verifications of numerical predictions for the hydrodynamic performance of horizontal axis marine current turbines," *Renewable Energy*, 32 (15), 2479-2490.

Bramwell, AR, Balmford, D, and Done, G (2001). *Bramwell's helicopter dynamics*. Butterworth-Heinemann.

Cheng, ZS, Madsen, HA, Chai, W, Gao, Z, and Moan, T (2017a). "A comparison of extreme structural responses and fatigue damage of semi-submersible type floating horizontal and vertical axis wind turbines," *Renew Energ*, 108, 207-219.

Cheng, ZS, Madsen, HA, Gao, Z, and Moan, T (2017b). "A fully coupled method for numerical modeling and dynamic analysis of floating vertical axis wind turbines," *Renew Energ*, 107, 604-619.

Henriques, JCC, Gato, LMC, Falcao, AFO, Robles, E, and Fay, FX (2016). "Latching control of a floating oscillating-water-column wave energy converter," *Renew Energ*, 90, 229-241.

Hu, ZQ, Li, L, Wang, J, Hu, QH, and Shen, MC (2016). "Dynamic responses of a semi-type offshore floating wind turbine during normal state and emergency shutdown," *China Ocean Eng*, 30 (1), 97-112.

Jonkman, JM (2010). *Definition of the Floating System for Phase IV of OC3*. Citeseer.

Jonkman, JM, and Buhl Jr, ML (2005). "FAST User's Guide", in: Secondary Jonkman, JM, and Buhl Jr, ML (Eds.). National Renewable Energy Laboratory (NREL).

Koo, BJ, Goupee, AJ, Kimball, RW, and Lambrakos, KF (2014). "Model Tests for a Floating Wind Turbine on Three Different Floaters," *J Offshore Mech Arct*, 136 (2), 020907.

Li, L, Gao, Y, Hu, Z, Yuan, Z, Day, S, and Li, H (2018a). "Model test research of a semisubmersible floating wind turbine with an improved deficient thrust force correction approach," *Renew Energ*, 119, 95-105.

Li, L, Gao, Y, Yuan, ZM, Day, S, and Hu, ZQ (2018b). "Dynamic response and power production of a floating integrated wind, wave and tidal energy system," *Renew Energ*, 116, 412-422.

Li, L, Hu, ZQ, Wang, J, and Ma, Y (2015). "Development and Validation of an Aero-hydro Simulation Code for Offshore Floating Wind Turbine," *J Ocean Wind Energy*, 2 (1), 1-11.

Michailides, C, Luan, C, Gao, Z, and Moan, T (2014). "Effect of flap type wave energy converters on the response of a semi-submersible wind turbine in operational conditions," *International Conference on Ocean, Offshore and Arctic Engineering*, American Society of Mechanical Engineers, V09BT09A014-V009BT009A014

Muliawan, MJ, Karimirad, M, and Moan, T (2013). "Dynamic response and power performance of a combined Spar-type floating wind turbine and coaxial floating wave energy converter," *Renew Energ*, 50, 47-57.

Nielsen, FG, Hanson, TD, and Skaare, B (2006). "Integrated dynamic analysis of floating offshore wind turbines," *25th International Conference on Offshore Mechanics and Arctic Engineering*, American Society of Mechanical Engineers, 671-679

Principle Power, 2017, http://www.principlepowerinc.com/.

Wan, L, Gao, Z, and Moan, T (2015). "Experimental and numerical study of hydrodynamic responses of a combined wind and wave energy converter concept in survival modes," *Coast. Eng*, 104, 151-169.

Zhang, L, Wang, SQ, Sheng, QH, Jing, FM, and Ma, Y (2015). "The effects of surge motion of the floating platform on hydrodynamics performance of horizontal-axis tidal current turbine," *Renew Energ*, 74, 796-802.

Zhang, XT, and Yang, JM (2015). "Power capture performance of an oscillating-body WEC with nonlinear snap through PTO systems in irregular waves," *Appl. Ocean Res*, 52, 261-273.